Fury: an experimental dynamo with anisotropic electrical conductivity

Thierry Alboussière*
Université Lyon 1, ENS de Lyon,
CNRS, Laboratoire de Géologie de Lyon,
69622 Villeurbanne, France

Franck Plunian
Université Grenoble Alpes, Université Savoie Mont Blanc,
CNRS, IRD, IFSTTAR, ISTerre,
38000 Grenoble, France

Marc Moulin
ENS de Lyon, CNRS, Laboratoire de Physique,
69364 Lyon, France
(Dated: May 31, 2022)

We report measurements of dynamo action in a new experimental setup, named Fury, based on the use of an anisotropic electrical conductivity. It consists in a copper rotor rotating inside a copper stator, electrically connected with a thin layer of liquid metal, galinstan. Grooves have been cut in the copper so that, at each point, electrical conductivity can be considered to be that of copper along two directions while it is zero along the third one. The configuration is efficient and dynamo action can be powered by hand. We have also used a motor with better control, enabling us to drive the rotor at specified velocity or torque functions of time. The structure of the axisymmetric magnetic field produced is found to be close to the numerical modelling using FreeFem++. The experimental dynamo behaves very nearly as expected for a kinematic (solid) dynamo, so that the threshold dynamo velocity cannot be exceeded, or only briefly. Putting more mechanical power in the rotor rotation leads to an increase in the magnetic field intensity, the magnetic energy being proportional to the extra mechanical power beyond threshold. In the transient following a step increase of torque, torsional oscillations have been observed in magnetic and angular velocity signals.

I. PREVIOUS DYNAMOS

Dynamos can refer to different machines and was historically used to designate a device transforming mechanical energy into continuous electric current (Gramme's or Siemens' dynamos for instance). The device had a permanent magnet, which was sometimes enhanced like an electromagnet to increase the efficiency of the conversion [1]. Here, by dynamo, we mean a device or a natural object producing a magnetic field from the motion of electrically conducting materials, in the absence of magnetized materials (or materials with magnetic properties in the strictest acceptance). Many planets and all stars have a self-generated magnetic field, whereas their internal temperature is above the Curie point, precluding any magnetic effect. In the literature, we can find similar experimental realizations, with solid or liquid electrical conductors.

According to the definition above, there have been four self-generated experimental dynamos published in the literature. One is a 'solid' dynamo [2, 3], the other three have used liquid sodium [4–6]. Soon after the first theoretical dynamo model [7], Lowes and Wilkinson [2] made an experimental version of it, consisting in two cylindrical electrically conducting rotors, rotating in cylindrical bores in a solid sphere (or a cube in the second version) and in electrical contact through a film of liquid metal (mercury). Both rotors and the sphere have been made of soft iron to increase the magnetic permeability by a factor 250 (150 in the second version), in order to lower the dynamo threshold in terms of angular velocities. Dynamo action was reached with approximatively 200 W of mechanical energy. It took time and effort before fluid dynamos were realized. In 2000, the experiments in Riga [4] and [5] showed that dynamo action was possible with liquid sodium. In Riga, a flow inspired from the Ponomarenko model [8] was set up: a turbine propelled the fluid with strong rotation in a pipe, the fluid was then channelled back around the pipe while its rotation was stopped using baffles [4]. Dynamo action was obtained with 100 kW and 1.5 cubic meter of sodium. In Karlsruhe, an arrangement of helical pipes produced an array of helical flows of the same sign. This is an approximation for the G.O. Robert's model [9]. With 1.6 m^3 of sodium and about 500 kW, a stationary magnetic field was produced [5].

* thierry.alboussiere@ens-lyon.fr

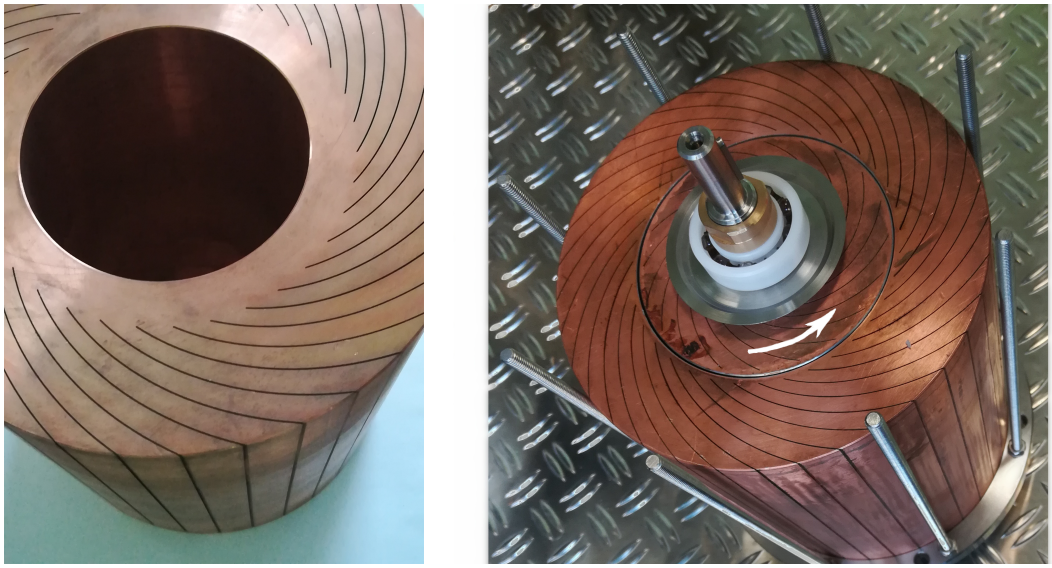

FIG. 1. Grooves are cut in a copper rotor and stator.

Finally, in Cadarache, the VKS experiment produced a dynamo effect in a cylinder with two counter-rotating discs at each end [6]. This arrangement can be seen as a realization of a Taylor-green vortex, although the flow becomes highly unsteady and turbulent for a moderate rotation rate of the discs. The discs had to be made of iron in order to reach the dynamo threshold. This setup required 160 liters of sodium and 150 kW for dynamo action.

With the more restrictive definition excluding magnetic properties, only two of the four experiments are dynamos. However, Riga and Karlsruhe dynamos are considered to be close to kinematic dynamos since the flow does not have much freedom to adapt to the self-generated magnetic field. On the contrary, the Cadarache dynamo is less constrained in terms of flow structure and a larger variety of non linear behaviours have been observed [10]. In all three cases, the mechanism of saturation above the threshold is not completely understood [4, 11, 12]. This is partly due to the fact that the setups have a limited amount of mechanical power and cannot reach velocities much above threshold, and partly due to the difficulty to detect very subtle changes in the velocity field.

II. FURY: FROM COPPER AND GROOVES

From our previous theoretical investigations on anisotropic electrical conductivity [13, 14], we know that a dynamo can have a planar velocity field and/or produce an axisymmetric magnetic field. We have built an experimental setup which is a rotor inside a stator (Fig. 1). The final external diameter of the stator is 170 mm, its length is 209 mm and its internal diameter is 101 mm. The rotor that fits inside has the same length and an external diameter of 100 mm, hence the gap between rotor and stator is 0.5 mm wide. It has an internal diameter of 30 mm so that a (non-magnetic) steel axis can be fitted in. The grade of copper for rotor and stator is CUA1 H12, with a guaranteed electrical conductivity σ between 100 and 102.5 % IACS, *i.e.* $\sigma = 5.8\ 10^7\,\Omega^{-1}m^{-1}$ to $\sigma = 5.95\ 10^7\,\Omega^{-1}m^{-1}$.

Grooves have been cut in the rotor and stator, extending across the whole length and forming arcs of logarithmic spirals in the perpendicular cross-section: the direction along the groove makes an angle 62 ° with the radial direction at all points. In the stator 35 equally-spaced spirals have been cut and 20 in the rotor. The grooves have been cut with the technique of electro-erosion, each groove has a width of 0.33 mm. The grooves have then been filled with a polyimide film and epoxy resin for electric insulation and mechanical strength. As can be seen on the left-hand side of Fig. 1, the internal diameter of the stator was cut 20 mm smaller initially to ensure rigidity during the cutting of the grooves (similarly, the external diameter of the rotor was larger by 20 mm). After the epoxy resin hardened, the stator internal and rotor external diameters were cut to the final dimensions, leaving a radial distance of 2 mm to the end of the grooves. This ensures a good precision and small roughness of the surfaces involved in the differential rotation. This surfaces (external of the rotor and internal of the stator) were then silver plated (a few microns) for chemical protection of the copper and to ensure good electrical contact with galinstan.

The assembly of the setup is quite simple, with two flanges at the top and bottom tied with threaded rods, ensuring mechanical cohesion with ball bearings inserted to hold the axis of the rotor. The gap between rotor and stator was

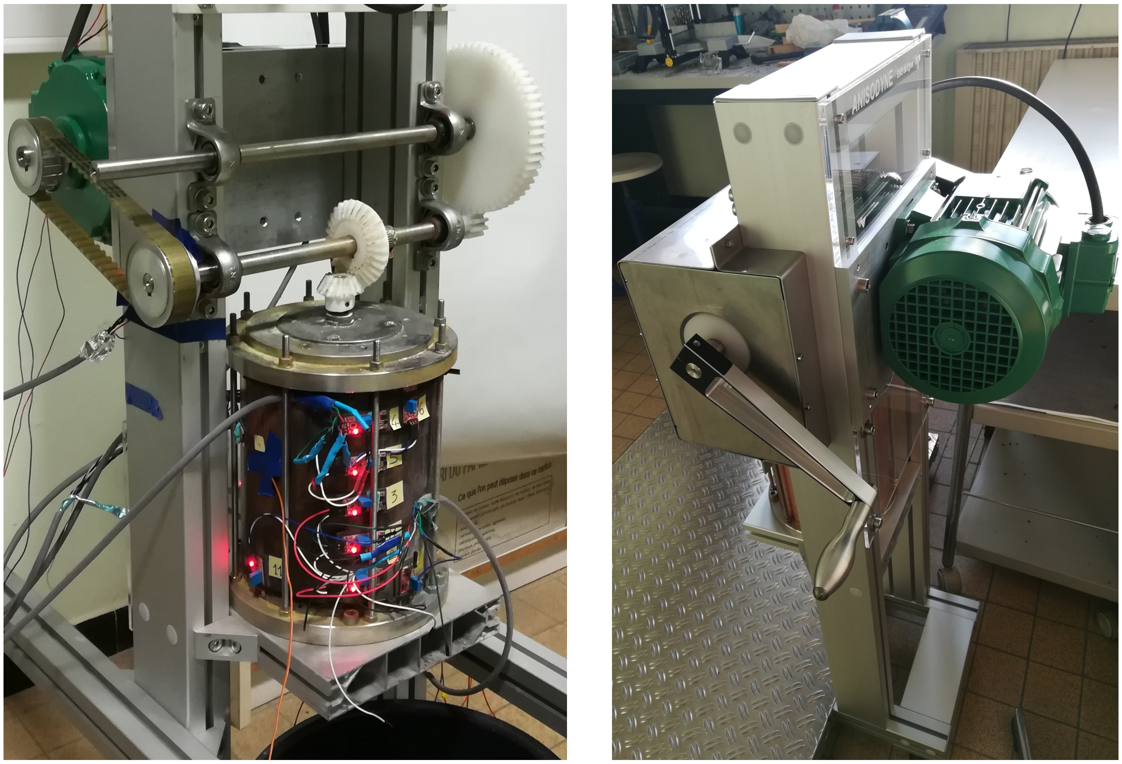

FIG. 2. Front view of Fury (left) and side view (right).

then filled with galinstan, an alloy of gallium, indium and tin, liquid at room temperature. In Fig. 2 showing the final setup, the copper stator is still visible and the rotor axis is connected through gears and belt to a handle and to an electric motor. Manual or motor operations are possible. One turn of the handle (resp. electric motor) corresponds to 12 (resp. 2) turns of the rotor axis.

Measurements are made of the magnetic field from Hall probes on the external surface of the stator: each Hall probes has a small red LED, see Fig. 2. The electric variator of the motor provides measurement of angular velocity and torque.

III. FURY: DYNAMO RESULTS

The dual operation, manual or motor-powered, has two distinct objectives. Powering the experiment by hand is interesting to have a direct physical feeling of dynamo action: one can feel the mechanical resistance due to Lorentz forces when the magnetic field is generated. However, the conditions of operation are not well controlled: the velocity is not constant nor the torque and is operator-dependent. Using a motor brings the possibility to follow almost any prescribed function of velocity or torque, within the limit of its maximal power.

A. The first successful human-powered dynamo run

The very first run of dynamo action with Fury took place on the 23rd of March 2021. In Fig. 3, one can see the signal of the two Hall probes (at the time) stuck on the outside of the stator. Those two signals are proportional to each other, although the two probes were at different places and had different orientations. This hints at the fact that the self-generated magnetic field is made of a single mode. Only its magnitude can change with time. Let us analyze the time evolution of this run. The operator ran the handle until it reached about 2 Hz, at a time between $t = 2$ s and $t = 3$ s. The magnetic field started to depart from its initial value (the ambient magnetic field). At the time nearly $t = 6$ s it peaked to a maximum. In the same time, the operator had experience an extra resistance from the Lorentz forces, which led to a decrease of the rotation rate and irregular decay of the magnitude of the magnetic

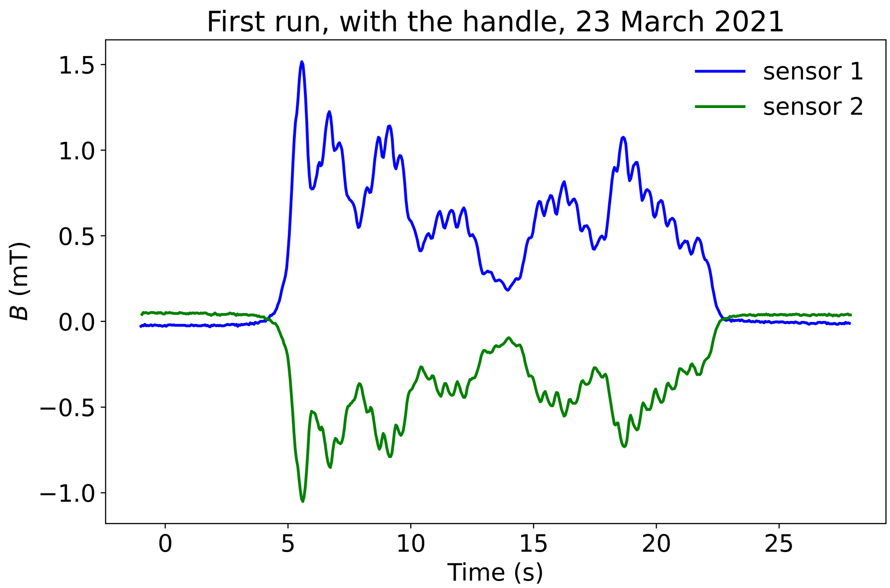

FIG. 3. First dynamo action with Fury, human-powered with the handle.

field. At $t = 13$ s, the operator recovered a little and put more effort for a while, then stopped at $t = 22$ s or so.

Another information from the signals in Fig. 3 is the presence of a 2 Hz oscillation. This is precisely the frequency of the handle rotation. The interpretation is that the input of energy is not constant over one rotation of the handle, which seems quite plausible. Note that the ratio between handle and rotor rotation is 12 (a factor 6 in the gears between the horizontal axes, see Fig. 2, and 2 in the conical gears on top of the rotor). This implies that the threshold for dynamo action corresponds to an angular velocity around 24 Hz for the rotor.

As will be seen later, reaching 2 Hz with the handle requires an input of 230 W of mechanical work to overcome the resistance of the galinstan film (main contribution), ball bearings and gears. This is quite an effort with a handle, but all operators over a representative sample of ten colleagues (two women, eight men) could do it. The good news is that the effort does not need to be sustained for a long time. Within 5 s, it is usually possible to sparkle the dynamo.

B. More results with a motor

Most results have been obtained with an electric motor of maximal power 750 W (about one horse power). This is just a little bit more than what the average human can do, but it can sustain it for longer and can adjust the effort very precisely.

1. Marginal eigenvector

Using FreeFem++ [15], we have computed the marginal eigenvalue and eigenvector at the lowest possible rotation rate. This eigenmode is axisymmetric and is shown on Fig. 4: the mesh used for the finite element calculations is shown in the background, the toroidal isovalues are shown with colour level in the conducting domain (rotor-galinstan-stator) and some field lines of the poloidal component are drawn. On the right-hand side of Fig. 4, the cylindrical radial component of the magnetic field is plotted along the profile `A-B` on the outside surface of the stator (blue curve). The black dots are measurements of the same profile on Fury. The grey region around each point corresponds to the uncertainty of position (± 2 mm and magnetic field ±5 % of the maximum value, mainly due to orientation errors of Hall sensors). These points correspond to different runs and to different azimuthal angles. Considering the accuracy of the measurements, there is no sign of departure from axisymmetry. The agreement between the calculated profile and the measurements is quite good: it seems that the experimental values are slightly shifted to the bottom compared to the odd calculated profile.

Let us now consider the value of the magnetic Reynolds number corresponding to marginal stability. Let us define

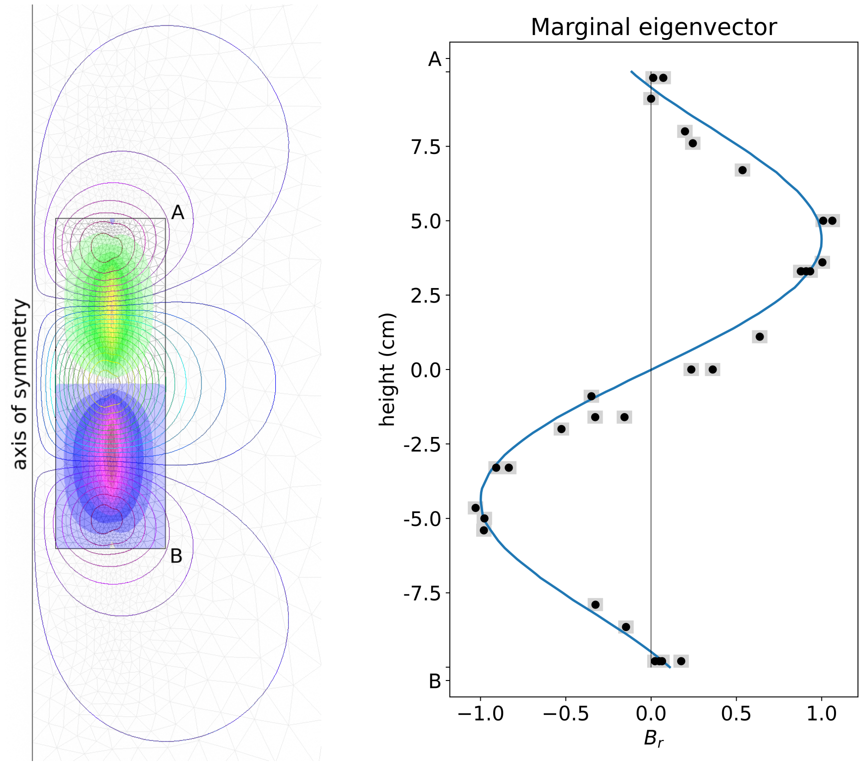

FIG. 4. Eigenmode at marginal stability from finite element modelling (FreeFem++) on the left, profile of B_r (FreeFem++ and measured on Fury) on the right.

the magnetic Reynolds number as $Rm = \mu\sigma UR$, with σ the electrical conductivity of copper, $\mu = 4\pi\,10^{-7}$ H m^{-1} the magnetic permeability of copper (or of vacuum), $R = 0.05$ m the radius of the rotor and $U = \omega R$ the maximal tangential velocity of the rotor (ω is the angular velocity). A rotation rate of the rotor of 24 Hz corresponds to an angular velocity of 150 rad s^{-1}. However, with the motor and more precise velocity measurements, we could get dynamo action for $\omega \simeq 147$ rad s^{-1} (green curve in Fig. 5). This leads to a critical magnetic Reynolds number of $Rm_c \simeq 26.8$. The dynamo threshold obtained with FreeFem++ is $Rm_c \simeq 23.1$. The difference can be explained firstly by the presence of a finite number of discrete grooves in the experiment, compared to a uniform anisotropy in FreeFem++ calculations. Secondly, the grooves correspond to a removal of about 5 % of the total mass of copper. This would already explain an increase by 5 % of the threshold. There can also be a contact electrical resistance between the copper and the film of galinstan. For completeness, the analytical threshold is $Rm_c \simeq 14.61$ with an infinitely long configuration and a stator of infinite radius (and in the absence of a layer liquid galinstan of electrical conductivity 16.76 times smaller than that of copper) [14].

2. Torque, power and magnetic energy

Increasing linearly the imposed torque from zero to its maximum value, we have been able to plot the resulting curves in the diagram shown in Fig. 5. Three runs in the “positive” direction of rotation are shown, and two in the reverse “negative” direction (see Fig. 1 where the white arrow defines positive rotation). In agreement with the mathematical analysis [13, 14] dynamo action is possible only with the positive direction of rotation. At low rotation rate, below the dynamo threshold, all curves follow the same path. The relationship between the angular velocity and the torque is determined by hydrodynamical properties of the galinstan alloy with additional torque contributions from the ball bearings (outside on the visible axes on Fig. 2, inside to support the axis of the rotor as shown in Fig. 1) and gears. The dashed black curve (original model) in Fig. 5 corresponds to the turbulent model by Orlandi *et al.* [16]. The continuous black curve (shifted model) is derived from the first one with a multiplication by 1.3 and with the addition of a constant resistive torque of 0.15 Nm, for a best fit of the data.

In the positive direction of rotation, above 150 rad s^{-1}, increasing further the torque does not result in an increase in angular velocity. The self-generated dynamo behaves pretty well like a kinematic dynamo: it is virtually impossible

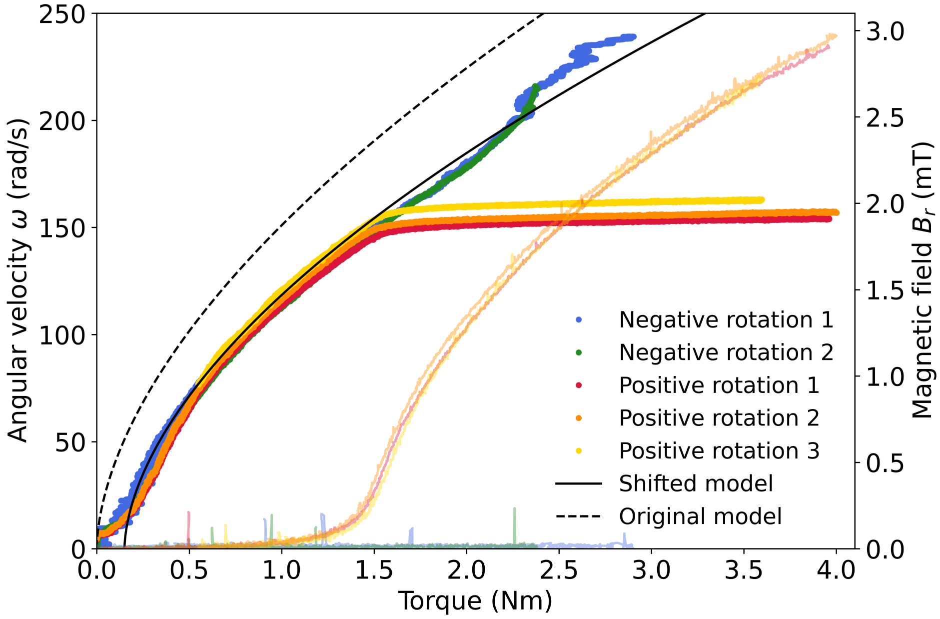

FIG. 5. Angular velocity and magnetic field (faded colours) versus torque, for two runs in the negative direction and three runs in the positive (dynamo) direction.

to exceed the threshold angular velocity (150 rad s^{-1} corresponds to $150/(2\pi) \simeq 24$ Hz). Increasing the torque leads to an increase in the self-generated magnetic field (fade colored curves in Fig. 5). On the contrary, in the negative direction of rotation, the same "hydrodynamical" curve is followed as for lower velocities and no magnetic field is generated.

In the dynamo regime (positive direction), a careful examination reveals that the angular velocity increases very slightly when the torque is increased above the threshold. However, most of this increase is due to the effect of temperature. As the system dissipates energy (by turbulence and viscosity at small scale, by Joule heating when the dynamo is running) the copper of the rotor and stator gets heated hence its electrical conductivity decreases. In order to maintain the kinematic dynamo at its critical magnetic Reynolds number, a decrease in electrical conductivity has to be compensated by a similar relative increase in angular velocity. In Fig. 5, the three dynamo runs, 1 to 3, were obtained while the temperature of the outside surface of the stator was 20.2, 22.4 and 25.6°C respectively. With a linear thermal coefficient of 4.3 10^{-3} K^{-1} for copper, the difference in temperature of 5.4 K leads to a relative variation of 2.3 % in electrical conductivity. The relative difference in angular velocity between run 1 and run 3 is about 5 %. We do not have a definite explanation for this mismatch: one possibility is that the temperature difference in the interior of the setup was larger than that measured on the external surface.

Anticipating on the next section III B 3, we can see in Fig. 7 that the magnetic energy grows linearly with the input mechanical power injected in the setup, when the dynamo threshold is exceeded. In that regime, any extra power input is dissipated by an extra Joule dissipation. This is coherent from the point of view of magnetohydrodynamics, as Joule dissipation scales usually proportionally to the square of the magnetic field for a given velocity field, in the magnetic diffusive regime.

3. Torque steps, torsional oscillations

When the experimental setup Fury is run with an electric motor, we can impose a torque and step changes over a very short duration of less than 0.1 s. In Fig. 6, we show the time evolution of an experiment where we have imposed 12 steps of increasing torque (labeled 1 to 12) and the reverse 12 steps of deceasing torque, in black continuous line. Each step duration is 10 s and the maximum torque was 4 Nm. As a result of these torque changes, angular velocity (blue line) increases significantly for the 5 first steps, then remains globally at the same level and finally goes down in the 5 last steps. After step 5 and until after step 19, self-exciting dynamo is at work, as shown by the value of the magnetic field (red curve), which maintains the angular velocity close to the dynamo threshold. The dynamo has

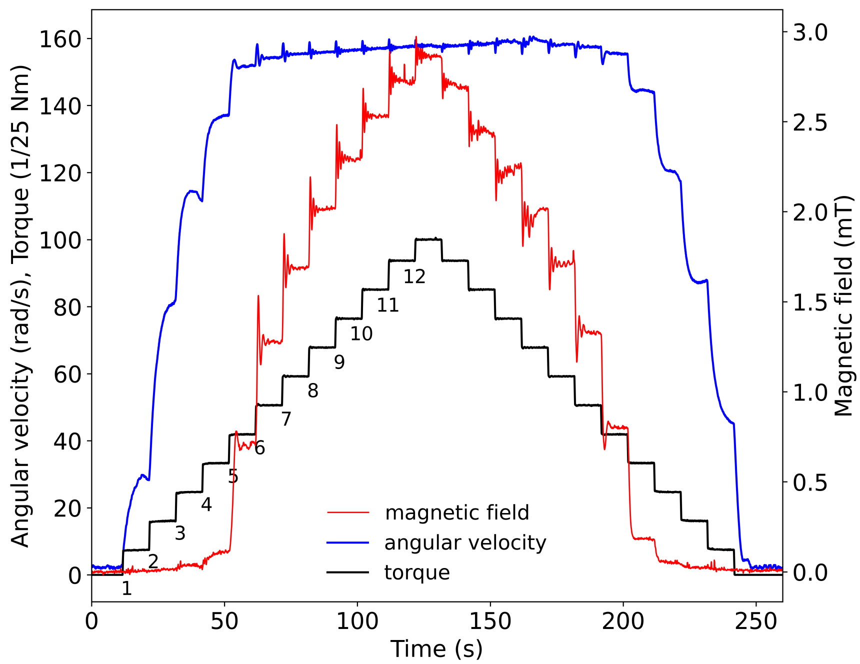

FIG. 6. Angular velocity, torque, magnetic field in a single run with imposed steps of torque in the positive direction of rotation.

actually perhaps started after the 4th step, as we can see a low level of magnetic field already. This is an indication that the dynamo threshold is not as sharp as expected for a kinematic dynamo, within a range of angular velocities, and we shall later explore this phenomenon.

In Fig. 7, the same experiment is represented in terms of mechanical energy input from the motor and square of the magnetic component B_r on the external surface of the stator (position $z = 3.7$ cm along the profile A-B in Fig. 4). In this diagram, the time evolution of the run is plotted in red while the torque is increased, then in blue for the second part of decreasing torque. In the dynamo regime, each step increase of the torque leads to an increase of mechanical power, followed by an increase of the magnetic energy. There is a transient phase of oscillations towards a final stationary regime where the path follows a converging spiral. The oscillations of the magnetic field can also be seen in Fig. 6 after each torque step. When the torque steps are in the decreasing phase (blue line), we observe a similar trend: the mechanical power goes down quickly and a phase of oscillating magnetic field follows with a final lower level of magnetic field. As mentioned above, the stationary points are well aligned along a straight line and we find a good agreement with the expression $B_r^2 = 0.0204(\mathcal{P} - 231)$ above the dynamo threshold (B_r in mT and the mechanical power input $\mathcal{P}$ in Watt).

It seems that the oscillations get faster as the magnetic field increases, in Fig. 6. We plot the oscillations following steps 5 to 12 in Fig. 8, using a dimensionless timescale proportional to the intensity of the magnetic field. Specifically, we use a timescale relevant to Alfvén waves, $tB_r/(R\sqrt{\rho\mu})$ with $R = 0.05$ m the radius of the rotor, $\rho = 8960$ kg m^{-3} copper density, $\mu = 4\,\pi\,10^{-7}$ H m^{-1} magnetic permeability and B_r (in Tesla) the limit radial magnetic field after each step. The oscillations of B_r superimpose nicely in this dimensionless timescale, and their period is of order one (close to 0.5). In the inset of Fig. 8, we have plotted again the magnetic signal after one of the steps (step 9), along with the signal of angular velocity fluctuations. Those signals are in phase quadrature relative to each other, similarly to Alfvén waves [17]. Because of the axisymmetry of the configuration and magnetic mode, these oscillations seem to be of the same nature of a particular kind of Alfvén waves, *i.e.* torsional oscillations. Such oscillations have been detected in the Earth's core [18] from geomagnetic data and also in an experiment with liquid sodium [19].

However, they are not Alfvén waves, nor associated torsional oscillations. Alfvén waves develop when kinematic and magnetic diffusion are negligible. Here, even with the highest magnetic field, the period of the oscillations is just under one second, while magnetic diffusion through 5 cm of copper is about 0.02 s. The oscillations are related to the dynamo mechanism itself: after a step, the system is pushed initially in the supercritical domain $Rm > Rm_c$ leading to a positive growth rate of the (global diffusive) magnetic field. The resulting increase of dissipative Lorentz forces brings the velocity down and the setup enters the subcritical domain $Rm < Rm_c$ with a deficit in Lorentz forces compared to the applied torque. The rotation increases and this is the start of a new period of the oscillations. The

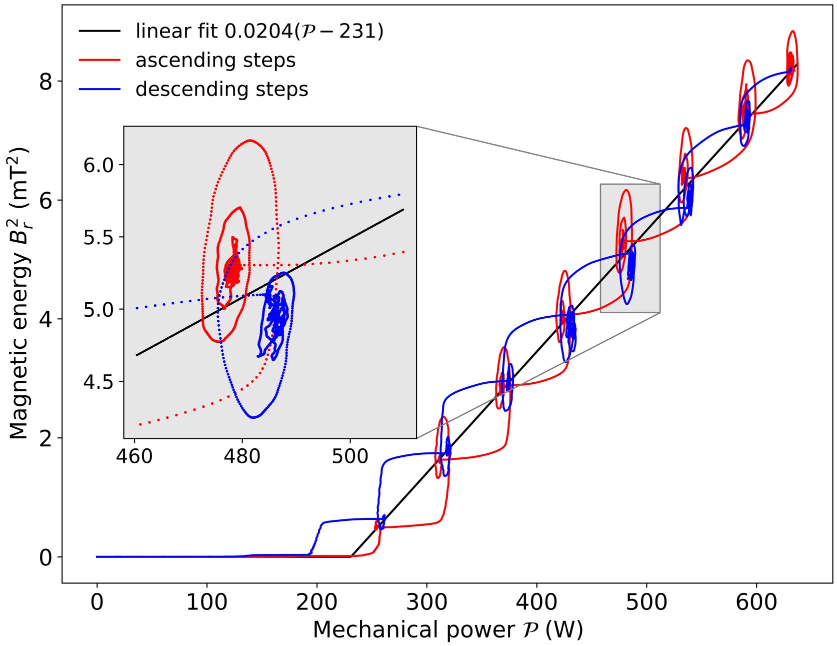

FIG. 7. Square of the measured magnetic field B_r^2 as a function of the mechanical power input $\mathcal{P}$ during the run shown in Fig. 6.

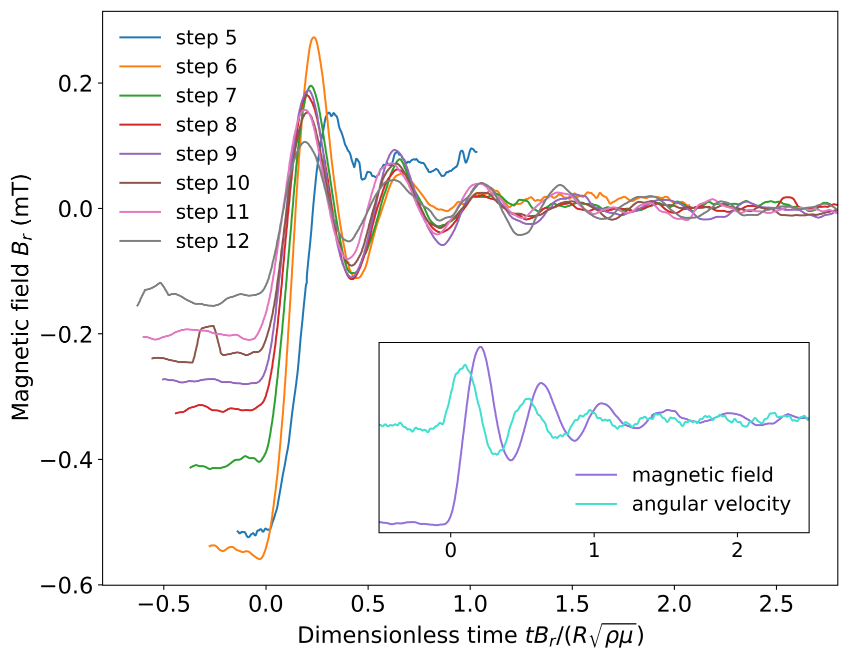

FIG. 8. Stack of magnetic field oscillations after steps of torque (see Fig. 6 for the numbering of steps) with the dimensionless time scale $tB_r/(R\sqrt{\rho\mu})$. The inset shows that the corresponding oscillations of angular velocity are in phase quadrature relative to magnetic oscillations, for step 9.

dynamic equation for the rotor rotation ω can be written approximately as follows

$$\rho R^2 \frac{\mathrm{d}\omega}{\mathrm{d}t} \simeq -\sigma\omega R^2 B_r^2 - \mathcal{T}_v + \mathcal{T}, \tag{1}$$

where $-\sigma\omega R^2 B_r^2$ is the Lorentz torque, $-\mathcal{T}_v$ the viscous torque and $\mathcal{T}$ the constant torque provided by the motor, per unit volume. Assuming the viscous torque to be constant, taking the time derivative leads to

$$\rho R^2 \frac{\mathrm{d}^2\omega}{\mathrm{d}t^2} \simeq -2\sigma\omega R^2 B_r \frac{\mathrm{d}B_r}{\mathrm{d}t} - \sigma R^2 B_r^2 \frac{\mathrm{d}\omega}{\mathrm{d}t}. \tag{2}$$

From our previous studies of the anisotropic dynamo, see equation (C17) of [13] and (4.18) of [20], we know that the growth rate of the magnetic field is proportional to $\omega - \omega_0$ (with a constant of order unity) near the dynamo threshold ω_0 for angular velocity. Substituting $\mathrm{d}B_r/\mathrm{d}t = (\omega - \omega_0)B_r$ in equation (2) and dividing by ρR^2, one obtains

$$\frac{\mathrm{d}^2(\omega - \omega_0)}{\mathrm{d}t^2} \simeq -2\frac{\sigma B_r^2}{\rho}\omega_0(\omega - \omega_0) - \frac{\sigma B_r^2}{\rho}\frac{\mathrm{d}(\omega - \omega_0)}{\mathrm{d}t}. \tag{3}$$

The last term on the right-hand side is negligible provided the timescale of the solution is longer than ω_0^{-1}. Making this assumption leads to a simple harmonic equation, of associated timescale $\tau = \sqrt{\rho/(\sigma\omega_0 B_r^2)}$ which is the geometric average of the (short) turnover timescale ω_0^{-1} and the (long) Joule damping time $\rho/(\sigma B_r^2)$. It is longer than ω_0^{-1}, hence our assumption is justified: it is also coherent with the smaller relative oscillations of angular velocity compared to those of the magnetic field in Fig. 6 after each step. This timescale τ can be expressed using $Rm_c = \mu\sigma\omega_0 R^2$ under the form

$$\tau = \frac{1}{\sqrt{Rm_c}}\frac{R}{V_A}, \tag{4}$$

where $V_A = B_r/\sqrt{\rho\mu}$ is the Alfvén velocity. This timescale τ is the timescale we have used to plot Fig. 8, without the constant $1/\sqrt{Rm_c} \simeq 1/5$. Even though the physics is different from that of Alfvén waves, a similar timescale arises from the coupling between rotor inertia and dynamo growth rate.

IV. CONCLUSIONS

We have demonstrated, with the experiment Fury, that the concept of anisotropic conductivity could be used effectively to produce a self-generated dynamo. Without any magnetic materials, just copper, and a small quantity of galinstan for thermal contact, we have built a dynamo that can be human-powered. The characteristics of the setup correspond rather well to the finite-element calculations, in terms of dynamo threshold and eigenmode of the magnetic field. Torsional oscillations have been put in evidence, due to the linear dynamo growth rate dependence around the threshold angular velocity.

Our measurements indicate that the magnetic field is axisymmetric. This cannot be exactly true: at small scale (smaller than the distance between the grooves), our setup is just made of materials of isotropic heterogeneous conductivity. So Cowling's theorems apply and an axisymmetric field cannot be sustained by dynamo action. So azimuthal variations must exist but they are small and we have not measured them yet. On a meso-scale (larger than the distance between the groove and smaller than the setup) we model the configuration by a material of homogeneous anisotropic electrical conductivity. In that case, axisymmetric dynamo solutions exist. Our results prove that this modelling is adequate for Fury.

A recent attempt to build a self-exciting dynamo with spiral arms was tested by Avalos-Zúñiga *et al.* [21]. The dynamo threshold was not reached because of technical problems, however it seems that an anisotropic conductivity would be a faithful model for this setup, too [22]. Concerning future experiments, one can imagine a hybrid solid-liquid configuration, similar to Fury but with a larger gap of liquid sodium, or just a solid anisotropic rotor inside a pool of liquid sodium. The advantage of these configurations is that dynamo action would be guaranteed from the solid anisotropic part and that fluid dynamics would interact non-linearly with the magnetic field. Considering the difficulties encountered to produce and study interesting non-linear dynamos, this alternative might be valuable.

The name Fury was given to the setup because this is a dynamo that should have the property of a dynamo growth-rate increasing without bound above the dynamo threshold, which we called a "very fast" or "furious" regime [13, 20]. That property is rather difficult to measure in the experiment because it would require a lot of mechanical power to maintain the setup at a velocity above the threshold velocity for a long enough period of time. We hope to make progress on this point in the future.

ACKNOWLEDGMENTS

We wish to acknowledge the participation of students of geology in Lyon, Lucie Petit, Dana Romanoz and Paul Gomez in the measurement of the magnetic profile of the dynamo mode. Thanks are due to Andy Jackson for suggesting the name 'Fury' for the setup. We thank the Programme National de Planétologie (PNP) of CNRS/INSU, co-funded by CNES. The authors are grateful to the LABEX Lyon Institute of Origins (ANR-10-LABX-0066) Lyon for its financial support within the program "Investissements d'Avenir" of the French government operated by the National Research Agency (ANR).

[1] H. Wilde, Experimental researches in magnetism and electricity, Philosophical Transactions of the Royal Society of London **157**, 89 (1867).
[2] F. J. Lowes and I. Wilkinson, Geomagnetic dynamo: A laboratory model, Nature **198**, 1158 (1963).
[3] F. J. Lowes and I. Wilkinson, Geomagnetic dynamo: An improved laboratory model, Nature **219**, 717 (1968).
[4] A. Gailitis, O. Lielausis, E. Platacis, S. Dement'ev, A. Cifersons, G. Gerbeth, T. Gundrum, F. Stefani, M. Christen, and G. Will, Magnetic field saturation in the Riga dynamo experiment, Physical Review Letters **86**, 3024 (2001).
[5] R. Stieglitz and U. Müller, Experimental demonstration of a homogeneous two-scale dynamo, Physics of Fluids **13**, 561 (2001).
[6] R. Monchaux, M. Berhanu, M. Bourgoin, M. Moulin, P. Odier, J.-F. Pinton, R. Volk, S. Fauve, N. Mordant, F. Pétrélis, A. Chiffaudel, F. Daviaud, B. Dubrulle, C. Gasquet, L. Marié, and F. Ravelet, Generation of a magnetic field by dynamo action in a turbulent flow of liquid sodium, Physical Review Letters **98**, 044502 (2007).
[7] A. Herzenberg, Geomagnetic dynamos, CERN Theoretical Study Division, Copenhague **250**, 543 (1958).
[8] Y. Ponomarenko, On the theory of hydromagnetic dynamos, Zh. Prikl. Mekh. & Tekh. Fiz. (USSR) **6**, 47 (1973).
[9] G. O. Roberts, Dynamo action of fluid motions with two-dimensional periodicity, Philosophical Transactions of the Royal Society of London. Series A, Mathematical and Physical Sciences **271**, 411 (1972).
[10] M. Berhanu, R. Monchaux, S. Fauve, N. Mordant, F. Pétrélis, A. Chiffaudel, F. Daviaud, B. Dubrulle, L. Marié, F. Ravelet, M. Bourgoin, P. Odier, J. F. Pinton, and R. Volk, Magnetic field reversals in an experimental turbulent dynamo, Europhysics Letters **77**, 59001 (2007).
[11] U. Müller, R. Stieglitz, and S. Horanyi, A two-scale hydromagnetic dynamo experiment, Journal of Fluid Mechanics **498**, 31 (2004).
[12] U. Müller, R. Stieglitz, and F. H. Busse, On the sensitivity of dynamo action to the system's magnetic diffusivity, Physics of Fluids **16** (2004).
[13] T. Alboussière, K. Drif, and F. Plunian, Dynamo action in sliding plates of anisotropic electrical conductivity, Physical Review E **101**, 033107 (2020).
[14] F. Plunian and T. Alboussière, Axisymmetric dynamo action is possible with anisotropic conductivity, Physical Review Research **2**, 013321 (2020).
[15] F. Hecht, New development in freefem++, J. Numer. Math. **20**, 251 (2012).
[16] P. Orlandi, M. Bernardini, and S. Pirozzoli, Poiseuille and Couette flows in the transitional and fully turbulent regime, Journal of Fluid Mechanics **770**, 424–441 (2015).
[17] T. Alboussière, P. Cardin, F. Debray, P. La Rizza, J.-P. Masson, F. Plunian, A. Ribeiro, and D. Schmitt, Experimental evidence of Alfvén wave propagation in a gallium alloy, Physics of Fluids **23**, 096601 (2011).
[18] N. Gillet, D. Jault, E. Canet, and A. Fournier, Fast torsional waves and strong magnetic field within the Earth's core, Nature **465**, 74 (2010).
[19] Z. Tigrine, H.-C. Nataf, N. Schaeffer, P. Cardin, and F. Plunian, Torsional Alfvén waves in a dipolar magnetic field: experiments and simulations, Geophysical Journal International **219**, S83 (2019).
[20] F. Plunian and T. Alboussière, Fast and Furious dynamo action in the anisotropic dynamo, Journal of Fluid Mechanics **941**, A66 (2022).
[21] R. A. Avalos-Zúñiga, J. Priede, and C. E. Bello-Morales, A homopolar disc dynamo experiment with liquid metal contacts, Magnetohydrodynamics **53**, 341 (2017).
[22] J. Priede and R. A. Avalos-Zúñiga, Feasible homopolar dynamo with sliding liquid-metal contacts, Physics Letters A **377**, 2093 (2013).